Spin coupling resonance and suppression in the AGS

V. H. Ranjbar and S. Y. Lee
Indiana University, Bloomington, Indiana 47405, USA

L. Ahrens, M. Bai, K. Brown, W. Glenn, H. Huang, A. Luccio, W. W. MacKay, V. Ptitsyn, T. Roser, and N. Tsoupas
Brookhaven National Laboratory, Upton, New York 11973, USA
(Received 6 December 2002; published 21 May 2004)

A spin matching method to cure intrinsic coupled spin resonances in the AGS is proposed and explored using an extension of the existing DEPOL program algorithm. The extension of DEPOL to handle linear coupling in the polarized beam acceleration is documented. Data collected from recent polarized proton experiments in the AGS are compared with the predictions derived from the extended DEPOL program.

DOI: 10.1103/PhysRevSTAB.7.051001 PACS numbers: 29.27.Hj, 29.20.–c

I. INTRODUCTION

The goal of the Relativistic Heavy Ion Collider (RHIC) spin project at Brookhaven National Laboratory is the delivery of polarized protons at the center of mass energies of 200–500 GeV. Polarized H^- ions from the Optically Pumped Polarized Ion Source [1] are accelerated to 200 MeV by a radio frequency quadrupole and a drift tube linac. They are then strip injected into the AGS Booster and accelerated to 1.5 GeV. The Alternating Gradient Synchrotron (AGS) accelerates polarized protons to 25 GeV and is the third stage in a complex of accelerators shown in Fig. 1. During injection in the AGS only one of the 12 rf buckets is filled and accelerated for the final injection into the RHIC with a typical bunch intensity of 1×10^{11} particles. A major bottleneck in the process of accelerating polarized protons occurs in the AGS. Because of the difficulty of preserving the polarization when accelerating through the spin-orbit resonances, the AGS accounts for most of the polarization losses. This paper describes work aimed at calculating and neutralizing these resonances. To understand these mechanisms it is necessary to understand the basics of spin motion.

The dynamics of the spin vector of a charged particle is determined by the interaction of the magnetic moment with the surrounding magnetic field. In the particle's rest frame this is described simply by

$$\frac{d\vec{S}}{dt} = \vec{\mu} \times \vec{B}, \tag{1}$$

where $\vec{S}$ is the spin vector of a particle and $\vec{\mu}$ is the magnetic moment. Transforming the fields to the laboratory frame, we obtain the TBMT equation (Thomas, Bargmann, Michel, and Telegdi) [2]

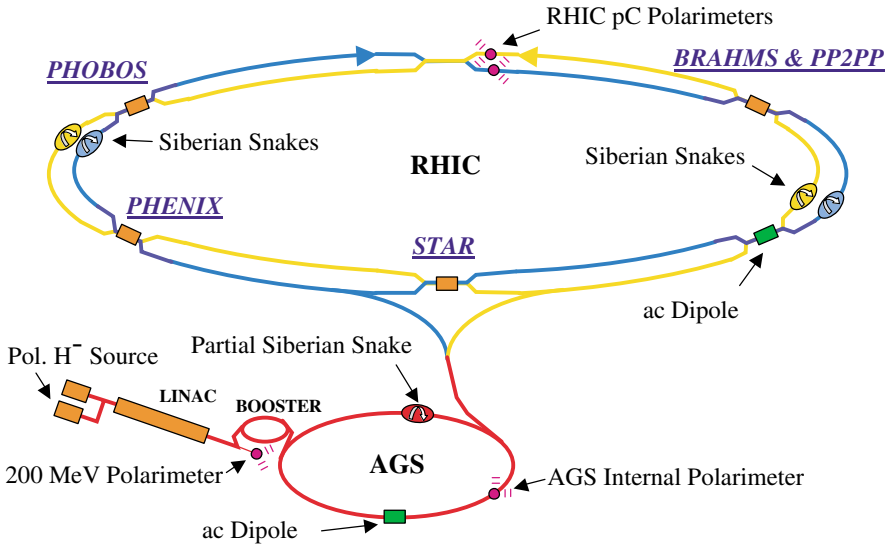

FIG. 1. (Color) The AGS-RHIC complex layout.

 1098-4402/04/7(5)/051001(13)$22.50

$$\frac{d\vec{S}}{dt} = \frac{e}{\gamma m}\vec{S} \times \left[(1 + G\gamma)\vec{B}_{\perp} + (1 + G)\vec{B}_{\parallel} + \left(G\gamma + \frac{\gamma}{\gamma + 1} \right) \frac{\vec{E} \times \vec{\beta}}{c} \right], \quad (2)$$

where the electromagnetic field vectors $\vec{E}$, $\vec{B}_{\perp}$, and $\vec{B}_{\parallel}$ are evaluated in the laboratory's frame relative to the direction of the particle's motion. $G = g - 2/2$ is the anomalous magnetic moment coefficient, and γmc^2 is the energy of the particle. However in reality the spin vector for a true spin-$\frac{1}{2}$ particle (i.e., an electron or proton in our case) should strictly speaking be treated quantum mechanically. But since we are not typically concerned with the spin state of a single particle but the ensemble average polarization in any given direction we define a polarization vector for a bunch with N protons as

$$\vec{P} = \frac{1}{N}\sum_{j=1}^{N} \frac{\vec{S}_j}{|S_j|}, \quad (3)$$

where $\vec{S}_j$ is the spin vector of the jth proton. The magnitude of polarization relative to the reference axis ξ is then given by

$$P = \hat{\xi} \cdot \vec{P}. \quad (4)$$

Since electric fields are normally small and parallel to the relativistic $\vec{\beta}$ vector, the TBMT equation becomes

$$\frac{d\vec{S}}{dt} = \vec{S} \times \vec{\Omega}, \quad (5)$$

where

$$\vec{\Omega} = \frac{e}{\gamma m}[(1 + G\gamma)\vec{B}_{\perp} + (1 + G)\vec{B}_{\parallel}] \quad (6)$$

has a magnitude of the spin precession frequency with its vector aligned along the axis of precession.

It is convenient to describe particle motion in the Frenet-Serret coordinate system shown in Fig. 2 , where $\hat{x}$, $\hat{s}$, and $\hat{z}$ are the unit basis vectors along the radially outward, the longitudinal, and the transverse vertical axes, respectively.

Following Courant and Ruth [3] we have picked $\hat{s}$ to point in the counterclockwise direction instead of the more common notation $(\hat{x}, \hat{y}, \hat{s})$ with $\hat{s}$ defined in the clockwise direction. Transforming Ω to the frame which rotates with the cyclotron frequency ω_c we obtain

$$\vec{\Omega}_{\mathrm{rs}} = [\Omega_x\hat{x} + \Omega_s\hat{s} + (\Omega_z - \omega_c)\hat{z}]. \quad (7)$$

The stable spin direction $\hat{n}_{\mathrm{co}}$ is given by the periodic solution to the TBMT equation on the closed orbit. In the absence of solenoidal fields, vertical bends, and misalignments, $\hat{n}_{\mathrm{co}}$ is vertical. In the laboratory frame we find that $\vec{\Omega} = (e/\gamma m)(1 + G\gamma)B_z\hat{z}$, where $\hat{z}$ is the unit basis vector in the vertical direction and B_z is the vertical guide field. The periodic solution for this ideal case defines the direction of equilibrium polarization. Since the particle traverses the accelerator at the cyclotron frequency $\omega_c = (e/\gamma m)B_z$, the spin tune, defined as the number of spin precessions about the stable spin direction per revolution on the design orbit, becomes

$$\nu_{\mathrm{sp}} = \frac{\Omega - \omega_c}{\omega_c} = G\gamma, \quad (8)$$

i.e., a spin vector will precess around the vertical direction $G\gamma$ times during each revolution.

Using the orbital angle θ as the independent variable in the local rotating system the TBMT equation becomes

$$\frac{d\vec{S}}{d\theta} = \frac{d\vec{S}}{dt}\frac{dt}{d\theta} = \frac{1}{\omega_c}\vec{S} \times \vec{\Omega}_{\mathrm{rs}} = -\frac{1}{\omega_c}\vec{\Omega}_{\mathrm{rs}} \times \vec{S} = \vec{\omega} \times \vec{S}. \quad (9)$$

In the formalism of quantum mechanics a spin-$\frac{1}{2}$ particle can be found in either the up or the down eigenstate

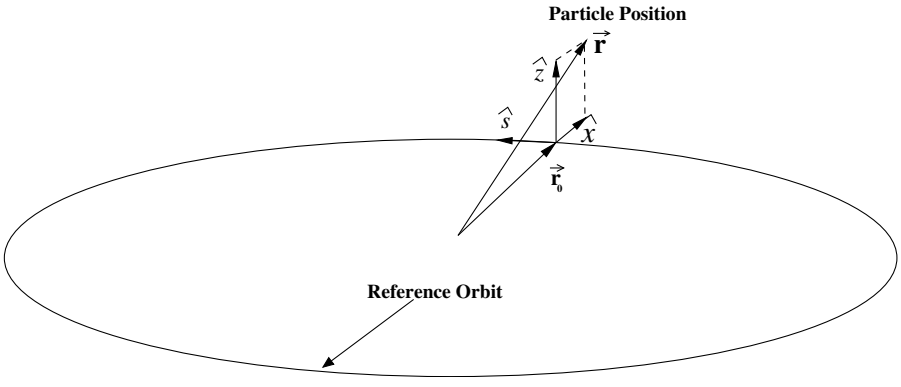

FIG. 2. The curvilinear coordinate system for particle motion in a synchrotron. Here $\hat{x}$, $\hat{s}$, and $\hat{z}$ are, respectively, the transverse radial, longitudinal, and transverse vertical unit basis vectors, and $\vec{r}_0$ is the reference orbit.

or in a coherent mixture of them with a certain probability distribution. Using a two component spinor with $\psi = \binom{u}{d}$, where u and d are the amplitudes for the particle to be in the two pure spin states and dropping the $\hbar/2$ units on S for the rest of the paper, we find

$$\vec{S} \equiv \langle\psi|\vec{\sigma}|\psi\rangle = \psi^\dagger \vec{\sigma}\psi, \tag{10}$$

where the components of $\vec{\sigma}$ are the usual Pauli matrices:

$$\sigma_x = \begin{pmatrix} 0 & 1 \\ 1 & 0 \end{pmatrix}, \quad \sigma_s = \begin{pmatrix} 0 & -i \\ i & 0 \end{pmatrix}, \quad \sigma_z = \begin{pmatrix} 1 & 0 \\ 0 & -1 \end{pmatrix}. \tag{11}$$

The TBMT equation of spin motion becomes

$$\frac{d\psi}{d\theta} = \frac{i}{2}(\vec{\sigma}\cdot\vec{\omega})\psi = \frac{i}{2}\begin{pmatrix} \omega_z, & \omega_x - i\omega_s \\ \omega_x + i\omega_s, & -\omega_z \end{pmatrix}\psi. \tag{12}$$

In an ideal case with $\omega_x = \omega_s = 0$, a solution to the TBMT equation is

$$\psi(\theta) = e^{-i(G\gamma/2)(\theta-\theta_0)\sigma_z}\psi(\theta_0) = t(\theta, \theta_0)\psi(\theta_0), \tag{13}$$

where $t(\theta, \theta_0)$ is the spin transfer matrix from azimuthal position θ_0 to θ. The spin transfer matrix in one revolution around the accelerator becomes

$$t(\theta_0 + 2\pi, \theta_0) = e^{-i\pi\nu_{\rm sp}\hat{n}_{\rm co}(\theta_0)\cdot\vec{\sigma}}. \tag{14}$$

Here $\hat{n}_{\rm co}(\theta_0)$ is vertical.

The AGS contains a partial snake. This is a solenoid which rotates a spin vector by an angle $\chi < 180°$ about the $\hat{s}$ direction per pass through the partial snake (a full 100% snake rotates the spin vector by $\chi = 180°$). The partial snake is an important device for reducing the depolarization at certain spin-orbit resonances. We describe its function in more detail later. The one-turn matrix for transforming the spinor wave function in the presence of the partial snake is

$$\begin{aligned}\psi(\theta_0 + 2\pi) &= e^{-i(G\gamma/2)(2\pi+\theta_0-\theta_{\rm sn})\sigma_z}e^{-i(\chi/2)\sigma_s} \\ &\quad\times e^{-i(G\gamma/2)(\theta_{\rm sn}-\theta_0)\sigma_z}\psi(\theta_0) \\ &= e^{-i\pi\nu_{\rm sp}\hat{n}_{\rm co}(\theta_0)\cdot\vec{\sigma}}\psi(\theta_0),\end{aligned} \tag{15}$$

where $\theta_{\rm sn}$ is the location of the partial snake. Solving for the spin tune $\nu_{\rm sp}$, we find that the spin tune is perturbed from $G\gamma$ as given by

$$\cos(\nu_{\rm sp}\pi) = \cos(G\gamma\pi)\cos\left(\frac{\chi}{2}\right). \tag{16}$$

The stable spin direction becomes

$$\begin{aligned}\hat{n}_{\rm co}(\theta_0) = \frac{1}{\sin\pi\nu_{\rm sp}}\Big(&- \sin[G\gamma(\pi + \theta_0 - \theta_{\rm sn})]\sin\frac{\chi}{2}\hat{x} \\ &+ \cos[G\gamma(\pi + \theta_0 - \theta_{\rm sn})]\sin\frac{\chi}{2}\hat{s} \\ &+ \sin(G\gamma\pi)\cos\frac{\chi}{2}\hat{z}\Big).\end{aligned} \tag{17}$$

If we let $\chi = r\pi$ with r representing the percentage of the snake used, at $G\gamma = m =$ integer, the spin tune becomes $m \pm \frac{r}{2}$. Thus the spin tune is shifted away from an integer by $\pm\frac{r}{2}$. In addition the stable spin direction is shifted which changes the average vertical polarization by

$$\langle S_z\rangle = P_{\rm inj}\left(\frac{\sin(\pi G\gamma)\cos(\frac{r\pi}{2})}{\sin(\pi\nu_{\rm sp})}\right)^2. \tag{18}$$

Here $P_{\rm inj}$ is our injected vertical polarization. For the data presented in this paper the snake strength ranged between $r \approx 3\%$–5%.

When a particle moves away from the "ideal orbit," the off-diagonal terms in Eq. (12) are no longer zero. By ideal orbit we mean the periodic orbit obtained without misalignments and which therefore goes through the centers of the quadrupoles. The perpendicular and parallel fields can be expressed using

$$\vec{B}_\perp = \frac{(\vec{v}\times\vec{B})\times\vec{v}}{v^2}, \qquad \vec{B}_\parallel = \frac{(\vec{v}\cdot\vec{B})\vec{v}}{v^2}. \tag{19}$$

Making use of the Lorentz force equation,

$$\frac{d\vec{v}}{dt} = \frac{e}{\gamma m}\vec{v}\times\vec{B}, \tag{20}$$

the perpendicular fields can be expanded in terms of derivatives with respect to s:

$$\vec{B}_\perp \approx \frac{p}{e}\left(1 - \frac{x}{\rho}\right)\left[\left(x'' - \frac{1}{\rho}\right)\hat{z} + \frac{z'}{\rho}\hat{s} - z''\hat{x}\right]. \tag{21}$$

Here ρ is the radius of curvature and $p = \gamma m v$ is the momentum of the beam which we have taken to be moving in the $\hat{s}$ direction (counterclockwise). For the parallel fields we find that the dominant terms which lie along the s direction are

$$\vec{B}_\parallel \approx (B_s + z'B_z)\hat{s}. \tag{22}$$

Assuming that $B(0)_s = 0$ and using Ampère's law, we obtain

$$\vec{B}_\parallel \approx -\frac{p}{e}\left(\frac{z}{\rho}\right)'. \tag{23}$$

$B(0)_s = 0$ is true for all elements except the partial solenoidal snake. In this case the spin perturbing effect of the partial solenoidal snake can be treated separately in the manner of Eq. (15). From the field expansions we can identify the elements of $\vec{\omega}$,

$$\begin{aligned}\omega_x &= -\rho z''(1 + G\gamma), \\ \omega_s &= (1 + G\gamma)z' - \rho(1 + G)\left(\frac{z}{\rho}\right)', \\ \omega_z &= -G\gamma + (1 + G\gamma)\rho x''.\end{aligned} \tag{24}$$

Depolarization due to spin-orbit resonances occurs if the fields drive the spin vector at a harmonic of the spin tune causing a spin depolarizing resonance condition. This most commonly happens during acceleration when the unperturbed spin tune $G\gamma$ ramps with energy and

crosses different resonant spin tunes. The spin resonance amplitude can be calculated by expanding the perturbing fields in a Fourier series:

$$\omega_x - i\omega_s = \sum_K \varepsilon_K e^{-iK\theta}, \tag{25}$$

where

$$\varepsilon_K = \frac{-1}{2\pi N_T}\int_0^{2\pi N_T}\Big[(1+G\gamma)(\rho z'' + iz') - i\rho(1+G)\Big(\frac{z}{\rho}\Big)'\Big]e^{iK\theta}d\theta. \tag{26}$$

Here K is the resonant spin tune, and the number of turns N_T depends on the rationality of K. If K is an integer then $N_T = 1$; however if K is an irrational number then we need an infinite number of turns. When calculating the resonant spin tune, the second term in ω_z is usually dropped since it is a small term compared to $G\gamma$. However this term can generate a set of important hybrid resonances around the sidebands of dominant spin resonances [4]. It is also worth pointing out that θ is constant in a region without dipoles; for this reason it is clearer to express Eq. (26) in terms of s:

$$\varepsilon_K = -\frac{1}{2\pi N_T}\int_0^{CN_T}\Big[(1+G\gamma)\Big(z'' + \frac{iz'}{\rho}\Big) - i(1+G)\Big(\frac{z}{\rho}\Big)'\Big]e^{iK\theta(s)}ds, \tag{27}$$

where C is the circumference of the ring.

The amount of depolarization caused by acceleration through any given spin resonance can be evaluated using the Froissart-Stora formula [5]

$$S_z = 2e^{-(\pi|\varepsilon_K|^2/2\alpha)} - 1, \tag{28}$$

where

$$\alpha = \frac{1}{\omega_{\rm rev}}\frac{d\nu_s}{dt} \tag{29}$$

is the spin tune crossing rate divided by the angular revolution frequency $\omega_{\rm rev}$, and S_z is the vertical component of the spin vector after passing through a spin resonance for an initially vertical spin. For a flat orbit in a constant vertical field $\alpha \simeq d(G\gamma)/d\theta$. Equation (28) represents a solution to the TBMT equation for the special case of crossing an isolated spin resonance. When $|\varepsilon_K|^2/2\alpha$ is large, a full spin flip can be induced to preserve polarization.

Spin depolarizing resonances in the AGS are of three main types: imperfection resonances, intrinsic resonances, and intrinsic coupled spin resonances. All three are predominately due to spin kicks accumulated from vertical beam motion through quadrupoles. They differ in the causes of the vertical motion. Imperfection resonances usually arise from vertical closed orbit distortions. Intrinsic resonances arise from vertical betatron oscillations. Intrinsic coupled spin resonances are derived from the projection of horizontal betatron oscillations in the vertical plane due to linear coupling. We can understand the motion of the beam around the ring by breaking up its motion into contributions from betatron motion z_β and closed orbit distortions $z_{\rm co}$ as

$$z = z_\beta + z_{\rm co}. \tag{30}$$

For the case of intrinsic resonances we use only the z_β piece to evaluate Eq. (26). The spin tune $\nu_{\rm sp}$ has a fractional part which requires that the integral be evaluated using $N_T \gg 1$. However in the perfectly decoupled case where the only coherent frequency is from the vertical betatron tune, the integral can still be calculated using only one turn by picking the appropriate exponential term from the cosine function in the betatron equation of motion. If we consider the effect of vertical betatron oscillations through quadrupole fields, the intrinsic resonance condition occurs when the spin tune obeys $\nu_{\rm sp} = m \pm \nu_z$, where m is an integer.

In the case of linear coupling the presence of two frequencies in the vertical motion requires more care. In addition, depolarizing fields arising from off-axis displacement through skew quadrupoles, vertical orbit correctors, and the fringes of the solenoid will contribute directly and indirectly via feed-down from sextupoles to both imperfection and intrinsic resonances. In Secs. III, we will treat this problem in detail. For the time being we note that since intrinsic coupled spin resonances arise from the normal-mode tune ν_u associated with the horizontal betatron tune ν_x, these resonances occur whenever $\nu_{\rm sp} = m \pm \nu_u \approx m \pm \nu_x$.

For imperfection resonances we use $z_{\rm co}$ to evaluate Eq. (26). Since K is an integer we need to use only one turn ($N_T = 1$). The effects of both partial and full snakes are calculated nonperturbatively in Eq. (15) so we need not calculate the zeroth order effect of the solenoidal partial snake.

There is one other class of spin resonances that is due to synchrotron motion. These resonances arise mainly from the kinematic effect of spin tune modulation. They occur at $\nu_{\rm sp} = K \pm m\nu_{\rm syn}$ where m is an integer, K is the tune of the primary resonance, and $\nu_{\rm syn}$ is the synchrotron tune. If the primary resonance strength is greater than the synchrotron tune, then synchrotron sidebands overlap with the primary resonance. This is the case for the AGS where $\nu_{\rm syn}$ is about 10^{-3}. Previous polarized proton experiments indicate that these resonances are not important at the spin tune crossing rate of $\alpha \approx 10^{-5}$ (see [6] for more detail).

Using Eq. (27) to calculate spin resonances assumes that $\hat{n}_{\rm co}$ is vertical. We also find resonances driven by longitudinal and radial fields. An extension of this approach to include $\hat{n}_{\rm co}$ that is tilted away from the vertical direction is not easily possible with this formalism. A

tilted $\hat{n}_{\rm co}$ requires a large horizontal field in the form of a partial or full Siberian snake or a spin tune close to an integer. In either case the integral in Eq. (26) will depend on N_T when K is not an integer. A proper treatment for cases where $\hat{n}_{\rm co}$ has large deviations from the vertical axis may not be treated by this perturbative formalism; however other approaches may permit a calculation with a tilted stable spin direction $\hat{n}_{\rm co}$ [7].

In recent years several novel methods to overcome the spin depolarizing resonances in the AGS have been pioneered. In 1994 a partial snake was installed and tested in the AGS [8]. The effect on the spin tune was shown in Eq. (16), where at every integer value of $G\gamma$ we see a discontinuity in the spin tune, and the spin tune becomes $m \pm (r\pi/2)$. The partial snake creates strong imperfection resonances at every integer K causing a spin flip. However, since the partial snake was built using a solenoid, strong coupling was introduced into the AGS, and the coupled spin resonances were enhanced.

In 1997, an ac dipole was installed and used to overcome strong intrinsic resonances in the AGS [9,10]. By driving the ac dipole near the vertical betatron tune to enhance the natural intrinsic resonance, a full spin flip is achieved. However, the ac dipole could not be used on the weak intrinsic resonances since the amplitude of the beam oscillation required to achieve a full spin flip was beyond the physical aperture of the AGS beam pipe.

Spin depolarizing resonances due to coupling may account for as much as a 30% loss of polarization in the AGS from the 70% injected. The major source of coupling in the AGS is the solenoidal snake. In the past some preliminary work was done to understand this phenomenon [11], and a method to overcome these resonances was attempted [12]. In the polarized proton run of 2002, the response of these coupled spin resonances to the strength of the solenoidal snake, skew quadrupoles, and vertical and horizontal betatron tune separations provided a benchmark for a modified DEPOL program [3].

To date, problems in the AGS remain with the weak intrinsic resonances and the coupled spin resonances. Problems with these resonances have hampered efforts to deliver the targeted 70% polarization to RHIC. So far the AGS has only been able to deliver a maximum of 40% polarization to RHIC. The polarized proton source during the 2002 run delivered protons polarized at 70% to the AGS Booster with 2×10^{11} particles per pulse. The polarized proton bunches were transferred to the AGS at $G\gamma = 4.6$ without polarization loss. Thus losses in the AGS amount to nearly 40% of the delivered polarization, all of which are due to the coupled and weak intrinsic resonances. A better understanding of the behavior of these resonances is urgently needed so that an effective remedy can be implemented.

This paper presents studies of spin matching correction in the AGS. Sections III extend the DEPOL algorithm to cover coupled spin resonances. A discussion of the AGS lattice and experimental setup is given in Sec. IV. Section V presents data gathered during the 2002 polarized proton run where the response of crossing the $0 + \nu_x$ coupled spin resonance was studied. These results are compared to the new DEPOL predictions. In Sec. VI, a new technique to suppress coupled spin resonances via spin matching with two families of skew quadrupoles rather than machine decoupling is presented. The conclusion is that by adding an additional family of skew quadrupoles the remaining coupled spin resonances can be suppressed.

II. TECHNIQUES FOR CALCULATION OF THE RESONANCE STRENGTH

As demonstrated previously the spin resonance strength for a vertically oriented spin vector can be calculated to first order using

$$\varepsilon_K = -\frac{1}{2\pi N_T}\int_0^{CN_T}\left[(1+G\gamma)\left(z'' + \frac{iz'}{\rho}\right) - i(1+G)\left(\frac{z}{\rho}\right)'\right]e^{iK\theta(s)}ds, \tag{31}$$

where C is the circumference of the ring, K is the resonance spin tune, ρ is the bending radius, x and z are the transverse horizontal and vertical components of the particle motion, θ is the orbit bending angle, and the independent variable s is the path length along the design orbit. Primes indicate derivatives with respect to s.

Although other algorithms [7] which address the problem of spin resonance calculation exist, owing to our familiarity with DEPOL, we proceed by building from its algorithm [3]. In DEPOL the strengths of imperfection and intrinsic resonances are evaluated by breaking up the integral in Eq. (31) into a sum over each element in the lattice

$$\varepsilon_K = \sum_{\rm lattice}\frac{\varepsilon_{K_m}}{N_T}, \tag{32}$$

$$\varepsilon_{K_m} = -\frac{1}{2\pi}\int_{s_1}^{s_2}\left[(1+K)\left(z'' + \frac{iz'}{\rho}\right) - i(1+G)\left(\frac{z}{\rho}\right)'\right]e^{iK\theta(s)}ds. \tag{33}$$

Assuming that $1/\rho$ is a step function, constant in the element and zero just outside the element, partial integration leads to an intermediate form,

$$\varepsilon_{K_m} = \frac{1}{2\pi}\left[\frac{(1+K)(\xi_1+i)}{\rho}z_1 e^{iK\theta_1} + \frac{(1+K)(\xi_2-i)}{\rho}z_2 e^{iK\theta_2} - (1+K)\int_{s_1}^{s_2} z'' e^{iK\theta}ds - \frac{K}{\rho^2}(K-G)\int_{s_1}^{s_2} z e^{iK\theta}ds\right]. \tag{34}$$

Here ξ_i is the contribution due to edge focusing of the magnet and $z_i = z(s_i)$. Applying partial integration again, we obtain

$$\varepsilon_{K_m} = \frac{1}{2\pi}\left\{\frac{(1+K)(\xi_1+i)}{\rho} z_1 e^{iK\theta_1} + \frac{(1+K)(\xi_2-i)}{\rho} z_2 e^{iK\theta_2} - (1+K)\left[\left(z_2' - \frac{iK}{\rho} z_2\right)e^{iK\theta_2} - \left(z_1' - \frac{iK}{\rho} z_1\right)e^{iK\theta_1}\right] + \left(\frac{K(K^2+G)}{\rho^2}\right)\int_{s_1}^{s_2} z e^{iK\theta} ds\right\}. \quad (35)$$

In the uncoupled case the integral is evaluated using the homogeneous equation $z'' = -K_z z$, where $K_z(s)$ is the focusing function of the guide field. Substitution using this equation allows an exact evaluation of Eq. (35).

In the case of linear coupling, however, the homogeneous equation is no longer valid for all the elements since z'' will depend not only on normal quadrupole fields but also on skew quadrupole fields and fields from vertical orbit correctors. In order to include the local spin perturbing effects arising from these radial fields we proceed by block diagonalizing the individual transfer matrices for the coupling elements. Thus we hope to transform the z coordinate into a basis where a new homogeneous equation is true. The technology to accomplish this has already been developed by Teng [13]. Given an element with off-diagonal values in the 4×4 transfer matrix:

$$\mathbf{M}_e = \begin{pmatrix} A_e & B_e \\ C_e & D_e \end{pmatrix}, \quad (36)$$

the 2×2 submatrices A_e, B_e, C_e, and D_e of the single element transfer matrix $\mathbf{M}_e$ can be used to develop a transformation which will block diagonalize $\mathbf{M}_e$. The result is

$$\mathbf{R}_e \mathbf{M}_e \mathbf{R}_e^{-1} = \begin{pmatrix} E_e & 0 \\ 0 & F_e \end{pmatrix}, \quad (37)$$

$$\mathbf{R}_e = \frac{1}{\sqrt{1+|r_e|}} \begin{pmatrix} I & -\bar{r}_e \\ r_e & I \end{pmatrix}, \quad (38)$$

$$\bar{r}_e = -\left(\frac{Tr(A_e - D_e)}{2} \pm \sqrt{|B_e + \bar{C}_e| + \frac{Tr^2(A_e - D_e)}{4}}\right)\frac{B_e + \bar{C}_e}{|B_e + \bar{C}_e|}. \quad (39)$$

The overbar on C indicates a symplectic conjugate, which is defined as

$$\bar{C} = -SC^T S, \quad (40)$$

with S being the matrix

$$S = \begin{pmatrix} 0 & 1 \\ -1 & 0 \end{pmatrix}. \quad (41)$$

Working with the canonical pairs $(x, p_x/p_s)$ and $(z, p_z/p_s)$ with $p_z/p_s \approx z'$ and $p_x/p_s \approx x'$ just outside the magnet, we can use $\mathbf{R}_e$ to transform them to a locally uncoupled basis a, a', b, and b':

$$\begin{pmatrix} x \\ x' \\ z \\ z' \end{pmatrix} = \mathbf{R}_e^{-1} \begin{pmatrix} a \\ a' \\ b \\ b' \end{pmatrix}. \quad (42)$$

In this basis the homogeneous equations $a'' = -K_a a$ and $b'' = -K_b b$ will hold. (Note that we absorb the sign which determines focusing or defocusing in the K_a and K_b variable.) We can determine focusing functions K_a and K_b by considering that most elements can have their transfer matrices cast in the form

$$\begin{pmatrix} a_2 \\ a_2' \end{pmatrix} = \begin{pmatrix} \cos(\varphi_a) & \frac{\sin(\varphi_a)}{\sqrt{K_a}} \\ -\sqrt{K_a}\sin(\varphi_a) & \cos(\varphi_a) \end{pmatrix}\begin{pmatrix} a_1 \\ a_1' \end{pmatrix}. \quad (43)$$

Thus $K_a = -(E_{e_{2,1}}/E_{e_{1,2}})$ and $K_b = -(F_{e_{2,1}}/F_{e_{1,2}})$. So to solve the integral in Eq. (35) we can write

$$z = [r_{e_{1,1}} a + r_{e_{1,2}} a' + b]\frac{1}{\sqrt{1+|r_e|}} \quad (44)$$

to obtain

$$\int_{s_1}^{s_2} z e^{ik\theta} ds = -\frac{1}{\sqrt{1+|r_e|}}\int_{s_1}^{s_2}\left[r_{e_{1,1}}\frac{a''}{K_a} + \frac{b''}{K_b} - r_{e_{1,2}} a'\right]e^{iK\theta} ds. \quad (45)$$

Now using an integration technique similar to the original DEPOL [3],

$$\int_{s_1}^{s_2} a'' e^{iK\theta} ds = \frac{(a_2' - \frac{iK}{\rho}a_2)e^{iK\theta_2} - (a_1' - \frac{iK}{\rho}a_1)e^{iK\theta_1}}{1 - K^2/K_a\rho^2} \quad (46)$$

we obtain a final closed expression:

$$\int_{s_1}^{s_2} z e^{iK\theta} ds = \frac{1}{\sqrt{1+|r_e|}}\left[\left(\frac{iK}{\rho} r_{e_{1,2}} - r_{e_{1,1}}\right)\left(\frac{(a_2' - \frac{iK}{\rho}a_2)e^{iK\theta_2} - (a_1' - \frac{iK}{\rho}a_1)e^{iK\theta_1}}{K_a - K^2/\rho^2}\right) - \left(\frac{(b_2' - \frac{iK}{\rho}b_2)e^{iK\theta_2} - (b_1' - \frac{iK}{\rho}b_1)e^{iK\theta_1}}{K_b - K^2/\rho^2}\right) + r_{e_{1,2}}(a_2 e^{iK\theta_2} - a_1 e^{iK\theta_1})\right]. \quad (47)$$

Thus our final expression for the resonance contribution from each element is

$$\varepsilon_{K_m} = \frac{1}{2\pi}\Bigg\{\frac{(1+K)(\xi_1+i)}{\rho}z_1 e^{iK\theta_1} + \frac{(1+K)(\xi_2-i)}{\rho}z_2 e^{iK\theta_2} - (1+K)\Bigg[\left(z_2' - \frac{iK}{\rho}z_2\right)e^{iK\theta_2} - \left(z_1' - \frac{iK}{\rho}z_1\right)e^{iK\theta_1}\Bigg] + \left(\frac{K(K^2+G)}{\rho^2}\right)\Bigg[\frac{1}{\sqrt{1+|r_e|}}\left(\left(\frac{iK}{\rho}r_{e_{1,2}} - r_{e_{1,1}}\right)\left(\frac{(a_2' - \frac{iK}{\rho}a_2)e^{iK\theta_2} - (a_1' - \frac{iK}{\rho}a_1)e^{iK\theta_1}}{K_a - K^2/\rho^2}\right)\right. - \left.\left(\frac{(b_2' - \frac{iK}{\rho}b_2)e^{iK\theta_2} - (b_1' - \frac{iK}{\rho}b_1)e^{iK\theta_1}}{K_b - K^2/\rho^2}\right) + r_{e_{1,2}}(a_2 e^{iK\theta_2} - a_1 e^{iK\theta_1})\right)\Bigg]\Bigg\}. \tag{48}$$

For those elements which are already block diagonal, we can neglect the local rotation to a diagonal basis and employ the original form

$$\int_{s_1}^{s_2} z e^{iK\theta} ds = \frac{(z_2' - \frac{iK}{\rho}z_2)e^{iK\theta_2} - (z_1' - \frac{iK}{\rho}z_1)e^{iK\theta_1}}{K_z - K^2/\rho^2}. \tag{49}$$

It should be noted that this algorithm does not take into account the effects of synchrotron sidebands, which in other machines can lead to an additional series of spin depolarizing resonances. In the AGS their effect can be neglected since the synchrotron sideband resonances merge with the main intrinsic resonance. Additionally we have neglected the effect arising from the change in the stable spin direction caused by the partial snake. For spin resonances away from the imperfection resonance condition, the spin vector is only slightly perturbed from its vertical direction. This algorithm does however account for multipole feed-down effects caused by closed orbit errors, provided that the software, which calculates the orbit, includes these effects in the transfer matrices.

III. IMPLEMENTATION OF NEW ALGORITHM

DEPOL uses Courant-Snyder parameters from the MAD [14] output files to construct the $z_{1,2}$ and $z'_{1,2}$ values necessary to evaluate the resonance amplitude. Yet when MAD evaluates the Courant-Snyder values under conditions of linear coupling, it employs u and v coordinates which correspond to the block diagonal basis for the one-turn transfer matrix. To correctly evaluate the resonance strength we must transform back to the original basis to obtain x, x', z, z'. So in the DEPOL code we read in values for the **R** matrix of the MAD output files and use it to transform the u, u', v, v' back to the x, x', z, z' basis. From here we can then implement Eq. (48) or (49) for each element.

Of course now one could directly calculate Eq. (31) by picking a sufficiently large value for N_T and evaluating it directly, but this would be computationally expensive. If we look closely at the behavior of the elements which make up the integral to be evaluated in Eq. (31), it appears that we can factor out the phase element which changes with each period around the lattice. The remaining elements in the sum remain constant for each pass. The factored phase elements can be evaluated analytically using the properties of a geometric series. This results in four separate functions called enhancement functions [6],

$$\begin{aligned} E_u(N_T)_\pm &= \sum_{n=0}^{N_T} e^{i2\pi n(K\pm\nu_u)} \\ &= \pm e^{iN_T\pi(K\pm\nu_u)}\frac{\sin(\pi(N_T+1)(K\pm\nu_u))}{\sin(\pi(K\pm\nu_u))}, \\ E_v(N_T)_\pm &= \sum_{n=0}^{N_T} e^{i2\pi n(K\pm\nu_v)} \\ &= \pm e^{iN_T\pi(K\pm\nu_v)}\frac{\sin(\pi(N_T+1)(K\pm\nu_v))}{\sin(\pi(K\pm\nu_v))}. \end{aligned} \tag{50}$$

Here ν_u and ν_v are the normal-mode betatron tunes, and N_T is the number of passes around the lattice. Each function, once evaluated, can then be multiplied by the appropriate terms in the sum over one pass in the lattice. The factors from Eq. (48) become

$$\begin{aligned} a_l e^{iK\theta_l} =& \left((\mathbf{R}_e\overline{\mathbf{R}})_{1,1}\frac{\sqrt{\beta(l)_u\epsilon_u}}{2} - (\mathbf{R}_e\overline{\mathbf{R}})_{1,2}\sqrt{\frac{\epsilon_u}{\beta(l)_u}}\frac{(\alpha(l)_u+i)}{2}\right)e^{i(K\theta_l - 2\pi\mu(l)_u)}E_u(N_T)_- \\ &+ \left((\mathbf{R}_e\overline{\mathbf{R}})_{1,1}\frac{\sqrt{\beta(l)_u\epsilon_u}}{2} - (\mathbf{R}_e\overline{\mathbf{R}})_{1,2}\sqrt{\frac{\epsilon_u}{\beta(l)_u}}\frac{(\alpha(l)_u-i)}{2}\right)e^{i(K\theta_l + 2\pi\mu(l)_u)}E_u(N_T)_+ \\ &+ \left((\mathbf{R}_e\overline{\mathbf{R}})_{1,3}\frac{\sqrt{\beta(l)_v\epsilon_v}}{2} - (\mathbf{R}_e\overline{\mathbf{R}})_{1,4}\sqrt{\frac{\epsilon_v}{\beta(l)_v}}\frac{(\alpha(l)_v+i)}{2}\right)e^{i(K\theta_l - 2\pi\mu(i)_u)}E_v(N_T)_- \\ &+ \left((\mathbf{R}_e\overline{\mathbf{R}})_{1,3}\frac{\sqrt{\beta(l)_v\epsilon_v}}{2} - (\mathbf{R}_e\overline{\mathbf{R}})_{1,4}\sqrt{\frac{\epsilon_v}{\beta(l)_v}}\frac{(\alpha(l)_v-i)}{2}\right)e^{i(K\theta_l + 2\pi\mu(l)_v)}E_v(N_T)_+, \end{aligned} \tag{51}$$

$$a_l' e^{iK\theta_l} = \left((\mathbf{R}_e \overline{\mathbf{R}})_{2,1} \frac{\sqrt{\beta(l)_u \epsilon_u}}{2} - (\mathbf{R}_e \overline{\mathbf{R}})_{2,2} \sqrt{\frac{\epsilon_u}{\beta(l)_u}} \frac{(\alpha(l)_u + i)}{2} \right) e^{i(K\theta_l - 2\pi\mu(l)_u)} E_u(N_T)_-$$
$$+ \left((\mathbf{R}_e \overline{\mathbf{R}})_{2,1} \frac{\sqrt{\beta(l)_u \epsilon_u}}{2} - (\mathbf{R}_e \overline{\mathbf{R}})_{2,2} \sqrt{\frac{\epsilon_u}{\beta(l)_u}} \frac{(\alpha(l)_u - i)}{2} \right) e^{i(K\theta_l + 2\pi\mu(l)_u)} E_u(N_T)_+$$
$$+ \left((\mathbf{R}_e \overline{\mathbf{R}})_{2,3} \frac{\sqrt{\beta(l)_v \epsilon_v}}{2} - (\mathbf{R}_e \overline{\mathbf{R}})_{2,4} \sqrt{\frac{\epsilon_v}{\beta(l)_v}} \frac{(\alpha(l)_v + i)}{2} \right) e^{i(K\theta_l - 2\pi\mu(i)_u)} E_v(N_T)_-$$
$$+ \left((\mathbf{R}_e \overline{\mathbf{R}})_{2,3} \frac{\sqrt{\beta(l)_v \epsilon_v}}{2} - (\mathbf{R}_e \overline{\mathbf{R}})_{2,4} \sqrt{\frac{\epsilon_v}{\beta(l)_v}} \frac{(\alpha(l)_v - i)}{2} \right) e^{i(K\theta_l + 2\pi\mu(l)_v)} E_v(N_T)_+, \quad (52)$$

$$b_l e^{iK\theta_l} = \left((\mathbf{R}_e \overline{\mathbf{R}})_{3,1} \frac{\sqrt{\beta(l)_u \epsilon_u}}{2} - (\mathbf{R}_e \overline{\mathbf{R}})_{3,2} \sqrt{\frac{\epsilon_u}{\beta(l)_u}} \frac{(\alpha(l)_u + i)}{2} \right) e^{i(K\theta_l - 2\pi\mu(l)_u)} E_u(N_T)_-$$
$$+ \left((\mathbf{R}_e \overline{\mathbf{R}})_{3,1} \frac{\sqrt{\beta(l)_u \epsilon_u}}{2} - (\mathbf{R}_e \overline{\mathbf{R}})_{3,2} \sqrt{\frac{\epsilon_u}{\beta(l)_u}} \frac{(\alpha(l)_u - i)}{2} \right) e^{i(K\theta_l + 2\pi\mu(l)_u)} E_u(N_T)_+$$
$$+ \left((\mathbf{R}_e \overline{\mathbf{R}})_{3,3} \frac{\sqrt{\beta(l)_v \epsilon_v}}{2} - (\mathbf{R}_e \overline{\mathbf{R}})_{3,4} \sqrt{\frac{\epsilon_v}{\beta(l)_v}} \frac{(\alpha(l)_v + i)}{2} \right) e^{i(K\theta_l - 2\pi\mu(i)_u)} E_v(N_T)_-$$
$$+ \left((\mathbf{R}_e \overline{\mathbf{R}})_{3,3} \frac{\sqrt{\beta(l)_v \epsilon_v}}{2} - (\mathbf{R}_e \overline{\mathbf{R}})_{3,4} \sqrt{\frac{\epsilon_v}{\beta(l)_v}} \frac{(\alpha(l)_v - i)}{2} \right) e^{i(K\theta_l + 2\pi\mu(l)_v)} E_v(N_T)_+, \quad (53)$$

$$b_l' e^{iK\theta_l} = \left((\mathbf{R}_e \overline{\mathbf{R}})_{4,1} \frac{\sqrt{\beta(l)_u \epsilon_u}}{2} - (\mathbf{R}_e \overline{\mathbf{R}})_{4,2} \sqrt{\frac{\epsilon_u}{\beta(l)_u}} \frac{(\alpha(l)_u + i)}{2} \right) e^{i(K\theta_l - 2\pi\mu(l)_u)} E_u(N_T)_-$$
$$+ \left((\mathbf{R}_e \overline{\mathbf{R}})_{4,1} \frac{\sqrt{\beta(l)_u \epsilon_u}}{2} - (\mathbf{R}_e \overline{\mathbf{R}})_{4,2} \sqrt{\frac{\epsilon_u}{\beta(l)_u}} \frac{(\alpha(l)_u - i)}{2} \right) e^{i(K\theta_l + 2\pi\mu(l)_u)} E_u(N_T)_+$$
$$+ \left((\mathbf{R}_e \overline{\mathbf{R}})_{4,3} \frac{\sqrt{\beta(l)_v \epsilon_v}}{2} - (\mathbf{R}_e \overline{\mathbf{R}})_{4,4} \sqrt{\frac{\epsilon_v}{\beta(l)_v}} \frac{(\alpha(l)_v + i)}{2} \right) e^{i(K\theta_l - 2\pi\mu(i)_u)} E_v(N_T)_-$$
$$+ \left((\mathbf{R}_e \overline{\mathbf{R}})_{4,3} \frac{\sqrt{\beta(l)_v \epsilon_v}}{2} - (\mathbf{R}_e \overline{\mathbf{R}})_{4,4} \sqrt{\frac{\epsilon_v}{\beta(l)_v}} \frac{(\alpha(l)_v - i)}{2} \right) e^{i(K\theta_l + 2\pi\mu(l)_v)} E_v(N_T)_+. \quad (54)$$

Here we are using the Courant-Snyder parameters $\beta(l)_{u,v}$ and $\alpha(l)_{u,v}$ evaluated at the l element in the $u - v$ basis. Also we use emittances $\epsilon_{u,v}$, the phase advance $\mu(l)_{u,v}$, and R is the one-turn rotation matrix. So we only need to evaluate the enhancement function to a sufficiently large value of N_T and then use factors derived above to evaluate Eq. (48). For our purposes we chose $N_T = 10\,000$. We found that for $N_T > 1000$ the enhancement factor converged with $|\delta\varepsilon_K| < 0.000\,001$ for a 10π mm-mrad emittance.

IV. EXPERIMENTAL SETUP

The AGS has 12 superperiods, each with 20 combined-function magnets to both bend and focus the beam around a ring of 807.12 m in circumference. A single superperiod can be seen in Fig. 3. In the AGS a partial solenoidal snake was employed to overcome imperfection resonances [8], and an ac dipole was used to overcome strong intrinsic resonances [9]. In past years the AGS was operated with a spin tune crossing rate of $\alpha = 4.8 \times 10^{-5}$. However, during the 2002 run a backup power supply was used to power the AGS main magnets resulting in a slower crossing rate of $\alpha = 2.4 \times 10^{-5}$. The lower acceleration rate allowed for a weaker partial snake since, at a slower acceleration rate, effective spin flipping due to the imperfection resonances is enhanced. Lowering the partial snake strength has the advantage of reducing the effective strength of the coupled spin resonances, but this is offset by an increase in the depolarization at all intrinsic resonance crossings, due to the slower acceleration rate. In the past, a 5% partial snake strength was used, but during this run a modified partial snake ramp was found to be the most effective. The current control of the partial snake was set up to maintain a 3% snake from injection to $G\gamma = 7.5$ and then to ramp up to 5% by $G\gamma = 21$. From $G\gamma = 21$ to extraction at $G\gamma = 46.5$ the snake was held at 5%.

The AGS is also equipped with a family of six skew quadrupoles each of which is located in the 17th straight section of every other superperiod, next to the horizontal tune quadrupoles. They are 0.390 88 m in length and the current can range from 0 to a maximum of 500 A which corresponds to $\int(\partial B_z/\partial z)ds = 0.84$ T.

V. STUDY OF COUPLING SPIN RESONANCES

The primary source of coupling in the AGS is the partial solenoidal snake. But it has been observed that

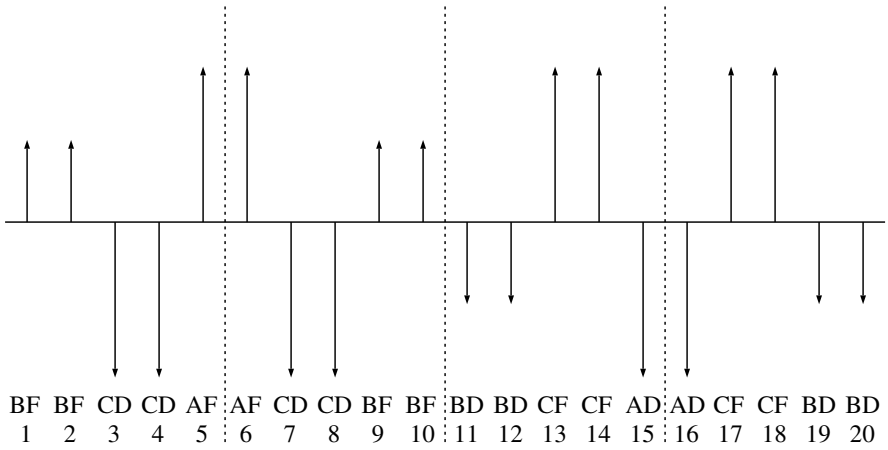

FIG. 3. AGS superperiod. Here up and down vectors show the direction and magnitude of the focusing gradient, and the letters denote the names assigned to each series of magnets.

the bare AGS machine has a net skew quadrupole component. Coupling studies in the past estimated the average roll per combined-function magnet to be 0.13 mrad [15]. Additionally closed orbit errors can contribute to coupling via feed-down from the sextupole fields present in the AGS combined-function magnets and sextupole magnets.

During the 2002 polarized proton run, particular attention was paid to studying the behavior of the $0 + \nu_u \approx 0 + \nu_x$ [16] resonance crossing during acceleration, since the analyzing power of the AGS polarimeter was sufficiently large at low energy to generate accurate measurements, and the strength of the $0 + \nu_u$ coupled spin resonance was large.

In Figs. 4–6, experimental data from scans of skew quadrupoles, horizontal tune, and the partial snake are compared with theoretical DEPOL calculations assuming a 70% polarization at injection into the AGS. In addition all emittances are given in terms of the normalized phase-space area containing 95% of the beam particles. All

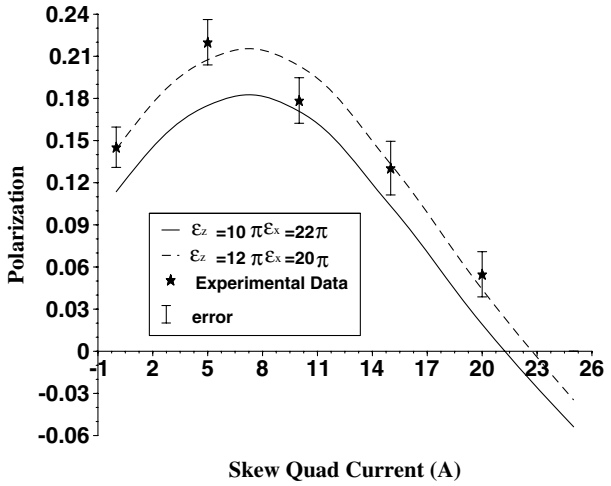

FIG. 4. Polarization after crossing the $0 + \nu_u$ and $0 + \nu_v$ resonances during acceleration with vertical and horizontal set-point normal mode tunes at $\nu_v = 8.8$ and $\nu_u = 8.78$ versus currents of all six skew quadrupole magnets. Snake strength was 3%. The vertical and horizontal emittances were measured as $(11 \pm 1)\pi$ and $(21 \pm 1)\pi$mm mrad. In addition, a distributed roll of <0.3 mrad was applied to the BD and CF magnets in the curves calculated using DEPOL.

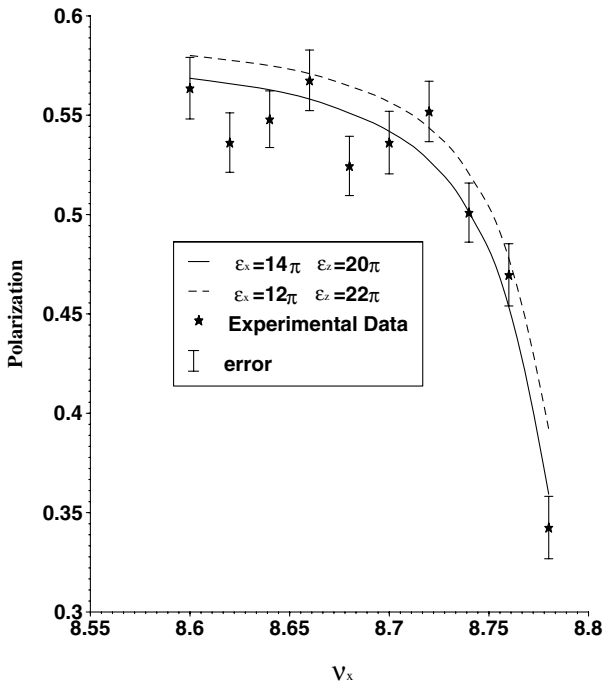

FIG. 5. Polarization after crossing the $0 + \nu_u$ and $0 + \nu_v$ resonances with set-point vertical normal mode tune ($\nu_v = 8.8$) versus horizontal set tunes. Snake strength was 3%. Vertical and horizontal emittances were measured as $(13 \pm 1)\pi$ and $(21 \pm 1)\pi$mm mrad, respectively. In addition, a distributed roll of <0.3 mrad was applied to the BD and CF magnets in the DEPOL calculated curves.

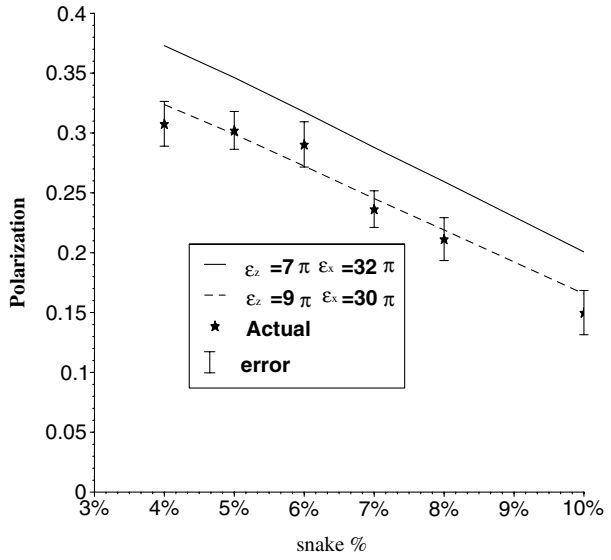

FIG. 6. Polarization after crossing the $0 + \nu_u$ and $0 + \nu_v$ resonances with fixed vertical and horizontal normal mode tunes ($\nu_v = 8.8$, $\nu_u = 8.7$) versus partial snake strength. Vertical and horizontal emittances were measured to be $(8 \pm 1)\pi$ and $(31 \pm 1)\pi$mm mrad. In addition, a distributed roll of <0.3 mrad was applied to the BD and CF magnets in the DEPOL calculated curves.

polarizations are calculated using

$$\frac{P_f}{P_i} = \frac{1 - \frac{\pi|\varepsilon_K|^2}{\alpha}}{1 + \frac{\pi|\varepsilon_K|^2}{\alpha}}. \tag{55}$$

This equation is the result of the integration of the Froissart-Stora formula over a Gaussian distribution. All tunes cited reflect the set-point tunes used in the AGS tune control program and not actual measured tunes. The control system does not account for the effect of the skew quadrupoles and solenoid. However for all the resonance calculations the correct tune shifts were calculated based on the currents sent to each magnet. Unless specified otherwise, the snake strength was set to 3%, the skew quadrupoles set to zero, and the ac dipole was turned off for Figs. 4–6. The results represent the net effect after acceleration through both the $0 + \nu_v \approx 0 + \nu_z$ and $0 + \nu_u$ spin resonances with an initial polarization of 70%.

The behavior demonstrated in these figures is consistent with the present understanding of intrinsic coupled spin resonances. An often-used analytical approximation to betatron motion in the presence of coupling is

$$z_\beta \approx \sqrt{\frac{\beta_z \epsilon_z}{\pi}} \cos(\nu_v \phi_z + \chi_z) + C_x \sqrt{\frac{\beta_u \epsilon_x}{\pi}} \cos(\nu_2 \phi_x + \chi_x), \tag{56}$$

where β_z and β_x are the unperturbed betatron amplitude functions, $\nu_{u,v}$ are normal-mode tunes, and $\chi_{z,x}$ are the z and x phases. The coupling coefficient is given by

$$C_x = \frac{|C_-|^2}{|\nu_x - \nu_z - l| + \sqrt{(\nu_x - \nu_z - l)^2 + |C_-|^2}} \tag{57}$$

with C_- being the integral of all the coupling elements in the ring (for more details see [17]). From Eq. (57) we can see that the coupling coefficient will depend on the separation of the horizontal and vertical tunes as well as the strength of the coupling elements. Since the magnitude of the intrinsic coupled spin resonance depends on the amplitude of the vertical oscillations due to the horizontal tune, this resonance should be directly proportional to the strength of the coupling coefficient. Naively we should expect, all things being equal, that a reduction in the coupling strength should lead to a reduction in the depolarization resulting from crossing an intrinsic coupled spin resonance. As we will discuss in the next section, this may not always be the case as it is possible for a globally decoupled machine with strong locally coupled regions to still have significant intrinsic coupled spin resonances.

Figure 5 shows that the polarization falls off as the tunes approach each other. Since the coupling coefficient by Eq. (57) is inversely proportional to the vertical and horizontal tune separations we expect the intrinsic coupled spin resonance strength to decrease with the tune separation, which is exactly what we observe.

In Fig. 6 we see that as the strength of the solenoidal snake increases, polarization falls off. This is due to the increase in coupling C_- caused by an increase in the solenoid strength. This in turn raised the amplitude of the associated intrinsic coupled spin resonance.

In Fig. 4, the behavior is a little more complicated. Net polarization first rises as the strength of the skew quadrupole is raised to 8 A and then declines as the current is raised above this value. Since the intrinsic coupled spin resonance strength is proportional to the coupling coefficient we believe that this behavior is due to the vectorial nature of the global coupling coefficient C_-. Since the solenoid has both imaginary and real contributions to C_- a single family of skew quadrupoles can cancel only the coupling component pointed in its direction. Thus at 8 A the skew quadrupole family only partially cancels the coupling caused by the partial snake.

Initial DEPOL calculations without rolls generated curves which were too broad. It was only by including either a large single roll or selectively placed rolls that a good fit to the measured data was achieved. For all DEPOL calculations shown here selectively distributed rolls were applied to the CF magnets [18] (0.05 mrad per magnet) and applied to the BD magnets [19] (0.25 mrad per magnet). This is not unreasonable considering previous estimates. However it should be emphasized that this configuration is by no means unique. While it was essential to include a net skew quadrupole component in the

bare AGS, the distribution and the direction of these rolls is still unclear since our data could fit many different configurations. Either the rolls of the magnets need to be surveyed, or a method similar to the "action phase jump technique" used in RHIC and in other machines could be used in the AGS [20–22].

VI. SUPPRESSION OF THE COUPLED SPIN RESONANCES

With the good agreement between experimental data and the DEPOL calculation demonstrated in Figs. 4–6 we can now proceed with confidence to consider ways to improve the surviving polarization in the AGS using DEPOL. One approach is to use an additional family of skew quadrupoles. In the AGS, there is a skew quadrupole at the 17th position of every other superperiod, i.e., six skew quadrupoles in total. They are currently used to help correct for the rolls in the combined-function bending magnets. On the basis of Eq. (57) one might be inclined to decouple the AGS globally. To do so ideally one should pick locations for additional skew quadrupoles with a large phase difference from the existing skew quadrupoles. The approach of global decoupling might succeed in yielding a small C_- but with sections of large skew and solenoidal fields the spin will still be perturbed as the particles oscillate horizontally through these sections.

Additionally, the field strength required for global decoupling causes a large tune shift which makes identifying the necessary strengths difficult, if not impossible. Since we are concerned with eliminating the coupled spin resonances and not necessarily decoupling the AGS, a spin matching condition may still exist. Harmonic spin matching has been used to date on weak intrinsic resonances in COSY and ELSA [23,24] and involves the introduction of a countervailing spin resonance perturbation which exactly cancels the existing spin resonances. To our knowledge, this technique has not been tried on intrinsic coupled spin resonances. It may be possible to either partly or totally cancel the intrinsic coupled spin resonance with the perturbation introduced by an additional set of skew quadrupoles that could be located just after dipole AD15 in every other sector. As shown in Figs. 7–10 we find that such a spin matching condition appears achievable for the four strongest intrinsic coupled spin resonances. We have fixed our vertical and horizontal normal-mode tunes ($\nu_v = 8.8$, $\nu_u = 8.7$) by adjusting the normal tune quadrupoles for each skew quadrupole setting. In this way the resonance location is fixed. These figures simulate the effect of scanning through various current strengths for skew quadrupoles in the 15th and 17th locations assuming an initial 100% polarization. A vertical emittance of 10π mm mrad was assumed with a spin tune ramp rate of α equal to 2.4×10^{-5} and the snake strength was set to 5%. For these calculations the new skew quadrupoles were assumed to have the same size and current-to-field transfer function as the existing skew quadrupoles in the 17th lattice position. For all four resonances a solution appears possible. However, overcoming the $36 + \nu_u$ resonance requires a current in excess of 1200 A. Since this high current needs to be maintained only during the brief time of the resonance crossing it should be possible. Actually a lower skew quadrupole current may in reality be sufficient since these calculations were all done assuming a spin tune ramp rate of $\alpha = 2.4 \times 10^{-5}$ generated by the backup Westinghouse main

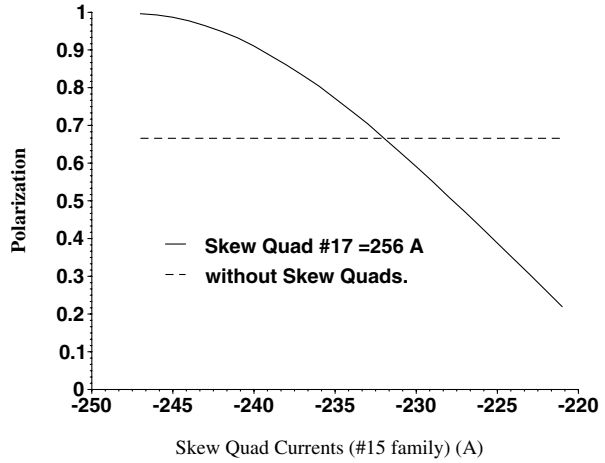

FIG. 7. Polarization after crossing the $0 + \nu_u$ resonance with fixed normal mode tunes ($\nu_v = 8.8$, $\nu_u = 8.7$) versus currents for hypothetical skew quadrupoles in the 15th straight sections. The 17th skew quadrupole family was fixed at 256 A. The dashed line indicates base polarization without any skew quadrupoles operating.

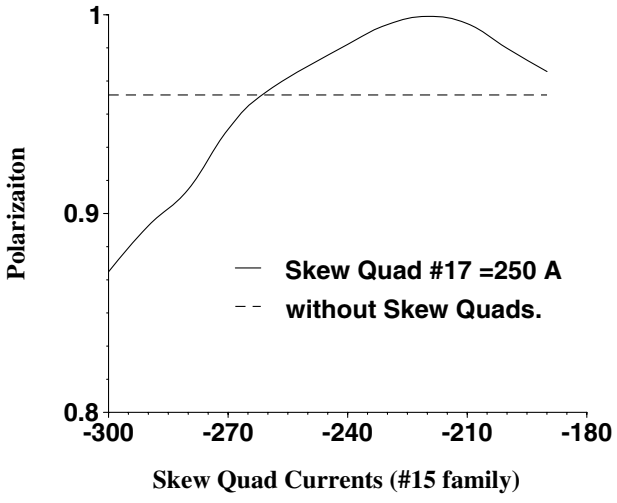

FIG. 8. Polarization after crossing the $12 + \nu_u$ resonance with fixed normal mode tunes ($\nu_v = 8.8$, $\nu_u = 8.7$) versus currents for hypothetical skew quadrupoles in the 15th straight sections. The 17th skew quadrupole family was fixed at 250 A. (The wiggle in the curve is due to an occasional failure of the MAD program to find the set tunes.) The dashed line indicates base polarization without any skew quadrupoles operating.

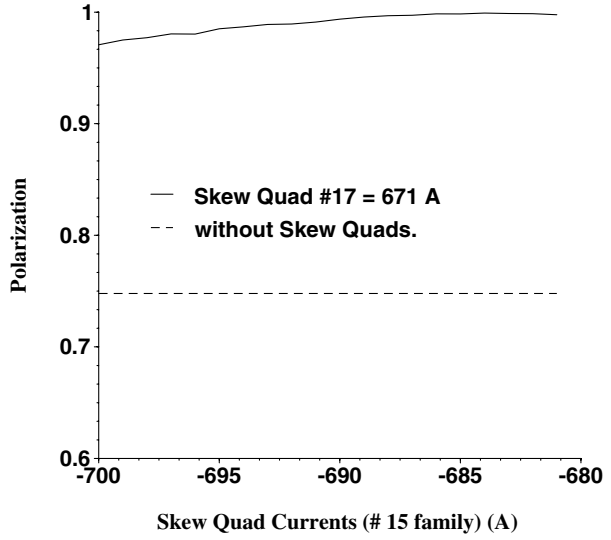

FIG. 9. Polarization after crossing the $36 - \nu_u$ resonance with fixed normal mode tunes ($\nu_v = 8.8$, $\nu_u = 8.7$) versus currents for hypothetical skew quadrupoles in the 15th straight sections. The 17th skew quadrupole family was fixed at 671 A. The dashed line indicates base polarization without any skew quadrupoles operating.

magnet power generator and not the usual rate of $\alpha = 4.8 \times 10^{-5}$, which is normally achieved by the Siemens main magnet power generator. Since the resonance strength as a function of skew quadrupole current has many local minima, we can most likely find a minimum at a lower skew quadrupole current with a stronger residual resonance. At the higher acceleration rate depolarization would still remain effectively zero.

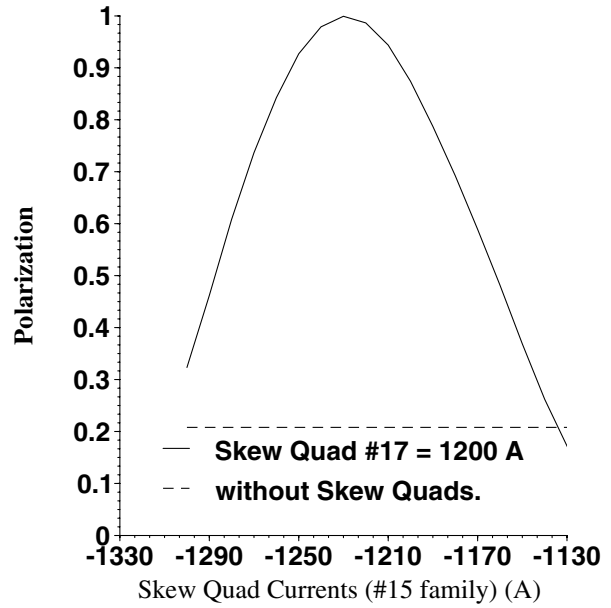

FIG. 10. Polarization after crossing the $36 + \nu_u$ resonance with fixed normal mode tunes ($\nu_v = 8.8$, $\nu_u = 8.7$) versus currents for hypothetical skew quadrupoles in the 15th lattice sections. The 17th skew quadrupole family was fixed at a current of 1200 A. The dashed line indicates base polarization without any skew quadrupoles operating.

VII. CONCLUSION

The 2002 polarized proton run in the AGS provided an opportunity to study the dependence of the $0 + \nu_u$ resonance strength on tune separation, skew quadrupole current, and snake strength. This study provides an experimental benchmark for the extended DEPOL. These results compared favorably with the new DEPOL calculations. Using the new DEPOL it has been shown that suppression of the coupled spin resonances in AGS can be achieved with the addition of a second family of six skew quadrupoles in the vacant 15th straight sections. A new helical superconducting strong partial snake [25] should provide a solution to the weak and strong intrinsic resonances and reduce coupling as compared with a solenoid. Our results in this paper show that a solution using a second family of skew quadrupoles with sufficient power should be capable of achieving a solution even in the most unfavorable relative phase location. Better results maybe achievable at other open lattice locations.

ACKNOWLEDGMENTS

This work was performed under the auspices of the U.S. Department of Energy, RIKEN of Japan, and Indiana University through Grants No. DOE DE-FG02-92ER40747 and No. NSF PHY-0140251.

[1] A. Zelenski *et al.*, Rev. Sci. Instrum. **73**, 888 (2002).
[2] L. H. Thomas, Philos. Mag. **3**, 1 (1927); J. Frenkel, Z. Phys. **37**, 243 (1926); V. Bargmann, L. Michel, and V. L. Telegdi, Phys. Rev. Lett. **2**, 435 (1959).
[3] E. D. Courant and R. D. Ruth, BNL Report No. 51270, 1980.
[4] M. Bai *et al.*, Phys. Rev. Lett. **84**, 1184 (2000).
[5] M. Froissart and R. Stora, Nucl. Instrum. Methods **7**, 297 (1960).
[6] S. Y. Lee, *Spin Dynamics and Snakes in Synchrotrons* (World Scientific, Singapore, 1997), pp. 36–39, 64–66, and 70–73.
[7] G. H. Hoffstaetter, Nucl. Phys. **A666–A667** 203c (2000).
[8] H. Huang *et al.*, Phys. Rev. Lett. **73**, 2982 (1994).
[9] M. Bai *et al.*, Phys. Rev. E **56**, 6002 (1997).
[10] M. Bai *et al.*, Phys. Rev. Lett. **80**, 4673 (1998).
[11] H. Huang, Ph.D. thesis, Indiana University, 1995.
[12] M. Bai and T. Roser, Report No. C-A/AP/37, 2001.
[13] L. C. Teng, FNAL Report No. FN 229, 1971.
[14] H. Grote and F. C. Iselin, CERN Report No. CERN/SL/90-13(AP), 1990.
[15] C. J. Gardner *et al.*, AGS Studies Report No. N224, 1987.
[16] Strictly speaking, in the presence of coupling, the intrinsic resonances are found at integers $\pm$ the eigentunes $\nu_{u,v}$; however we may approximate the normal-mode tunes by $\nu_u \approx \nu_x$ and $\nu_v \approx \nu_z$.

[17] G. Guignard, CERN Report No. 76-06, 1976.
[18] CF is the label for a family of combined-function focusing magnets located at 13, 14, 17, and 18 positions in each superperiod.
[19] BD is the label for a family of combined-function defocusing magnets located at 11, 12, 19, and 20 positions in each superperiod.
[20] F. Pilat *et al.*, in *Proceedings of the EPAC2002, Paris* (EPS-IGA/CERN, Geneva, 2002), p. 1178.
[21] J. Y. Liu *et al.*, Phys. Rev. E **49**, 2347 (1994).
[22] S. Y. Lee, *Accelerator Physics* (World Scientific, Singapore, 1999).
[23] C. Steier and D. Husmann, in *Proceedings of the 6th EPAC98, Stockholm, Sweden* (IOP, Bristol, U.K., 1998), p. 1033.
[24] A. Lehrach *et al.*, Nucl. Instrum. Methods Phys. Res., Sect. A **439**, 26 (2000).
[25] H. Huang *et al.*, AIP Conf. Proc. **667**, 209 (2002).